

J. D. Achenbach, A. K. Gautesen and H. McMaken  
 Technological Institute  
 Northwestern University  
 Evanston, Illinois 60201

#### ABSTRACT

The direct problem of the diffraction of time-harmonic waves by cracks in elastic solids is analyzed for high-frequencies, when the wavelengths are of the same order of magnitude as a characteristic length dimension,  $a$ , of the crack. It is shown that good approximations at high frequencies can be obtained on the basis of elastodynamic ray theory. An elastodynamic version of geometrical diffraction theory is briefly reviewed. We also present a hybrid theory, wherein the crack opening displacement is computed on the basis of geometrical diffraction theory, and the scattered field is subsequently obtained by the use of a representation theorem. This hybrid approach avoids the difficulties at shadow boundaries and caustic surfaces that plague a direct application of geometrical diffraction theory. Explicit results are computed for slits and penny-shaped cracks, and these results are compared with numerical results obtained on the basis of exact integral equation formulations. The relatively simple structure of the expressions for the scattered fields displays some characteristic features, whose possible role in the inverse problem is discussed.

#### INTRODUCTION

Experimental apparatus for quantitative flaw definition by the ultrasonic pulse method generally includes instrumentation to gate-out and spectrum analyze the various components of the signal diffracted by a flaw. After the scattering data have been corrected for transducer transfer functions and other characteristics of the system, amplitudes and phase functions are obtained, as functions of the frequency and the scattering angle. Such processed experimental data can then be compared with theoretical results.

For short pulses the frequency spectrum is centered in the high frequency (short wavelength) range. In this paper we present analytical results for diffraction of high frequency time harmonic waves. We consider frequencies corresponding to wavelengths that are of the same order of magnitude as the dominant cross-sectional dimension of the flaw. When the probing wavelength is that short, there are many interference processes, whose characteristic forms can provide the basis for an inversion procedure. A study of the direct problem is a necessary preliminary to the solution of the inverse problem, to generate understanding of the structure of the high-frequency diffracted field.

In this report we present analytical results that have been obtained by an approximate method which is based on elastodynamic ray theory.

Elastodynamic ray theory was presented in some detail by Karal and Keller<sup>1</sup>. The reflection of ray-carried signals at a boundary is well understood. The application of ray theory to diffraction by smooth obstacles has also been investigated in some detail, see e.g., Resende<sup>2</sup>. Reference 2 also appears to be the first one to deal with diffraction by a crack edge, at least in a two-dimensional geometry. A three-dimensional ray theory for diffraction by cracks has recently been discussed in some detail by Achenbach, Gautesen and McMaken<sup>3-6</sup>. The work presented in 3 is an extension to elastodynamics of geometrical

diffraction theory, which was introduced by Keller<sup>7</sup> for acoustic and electromagnetic diffraction problems. Geometrical diffraction theory has been extensively applied in electromagnetic scattering, see e.g. 8 and 9. The elastodynamic version of geometrical diffraction theory provides relatively simple results, and it can be applied to cracks of complicated shape. The theory is applicable if  $\omega a/c_l$  is sufficiently larger than unity, where  $\omega$  is the circular frequency,  $a$  is a characteristic dimension of the crack, and  $c_l$  is the velocity of longitudinal waves.

#### HIGH FREQUENCY THEORY

At high frequencies the diffraction of elastic waves by cracks can be analyzed conveniently on the basis of elastodynamic ray theory. For time-harmonic wave motion, ray theory provides a method to trace the amplitude of a disturbance as it propagates along a ray. In a homogeneous, isotropic, linearly elastic solid the rays are straight lines, which are normal to the wavefronts. An unbounded solid can support rays of longitudinal and transverse wave motion. In this paper these rays are denoted as L-rays and T-rays, respectively. The free surface of a solid can, in addition, support rays of surface-wave motion, which are denoted as R-rays.

In analogy with geometrical optics, the simplest theory for diffraction of elastic waves by cracks may be called geometrical elastodynamics (GE). In GE a crack acts as a screen, which creates a shadow zone of no motion, and zones of reflected waves. The shadow zone is bounded by all rays passing through the source point and the edge of the crack. The geometrical reflections of these rays bound the zone(s) of reflected rays. The displacement field according to GE, is of the same order of magnitude as the incident field. The GE-field is, however, physically unrealistic, because of discontinuities at the boundaries of the shadow zone and the zone(s) of reflected waves.

The geometrical theory of diffraction (GTD) provides a first correction to GE. This correction is valid for  $\omega a/c_L \gg 1$ , and at points where  $S/a > 1$ . Here  $\omega$  is the circular frequency,  $a$  is a length dimension of the crack,  $c_L$  is the velocity of longitudinal waves, and  $S$  is the distance from a crack edge. The correction provided by GTD is of order  $(\omega a/c_L)^{-1/2}$ .

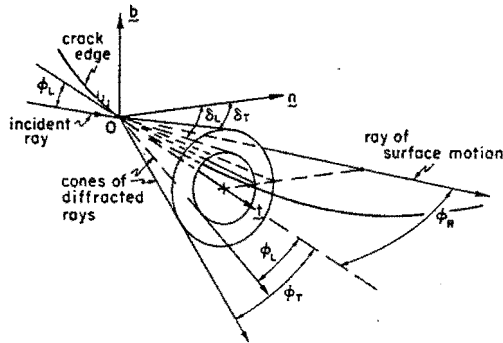


Fig. 1. Diffracted surface-wave ray and cones of diffracted body-wave rays.

Basic to GTD is the result that the incidence of a body-wave ray on the edge of a crack gives rise to two cones of diffracted body-wave rays and two R-rays (one on each crack face), see Fig. 1. The surfaces of the inner and outer cones of body-wave rays consist of L-rays and T-rays, respectively. When an R-ray intersects the edge of a crack, a ray of reflected surface wave motion is generated, as well as cones of diffracted body-wave rays.

With GE and GTD the total displacement field is still not valid at the boundaries of the shadow zone and the zone(s) of reflected waves. In a further refinement which is called uniform asymptotic theory (UAT), the fields at these boundaries are corrected. For some details on UAT we refer to Ref. 5.

For incident waves with curved wavefronts and for curved diffracting edges, the cones of diffracted rays have envelopes, at which the rays coalesce and the fields become singular. The envelopes are called caustics, and GTD breaks down at caustics.

**Summary of GDT Results.** Geometrical diffraction theory is based on the use of canonical solutions, which are asymptotic results for diffraction of a plane wave by a semi-infinite crack. In geometrical diffraction theory these canonical solutions are appropriately adjusted to account for curvature of incident wavefronts and curvature of crack edges, and for finite dimensions of the crack. For an incident longitudinal wave, the pertinent canonical solutions have been obtained by Achenbach et al, see Refs. 3 and 4,

Within the context of the GTD theory of Refs. 3 and 4, the diffracted field at a point of observation  $Q$  is comprised of contributions correspond-

ing to "primary" diffracted body-wave rays, which are directly generated by incident body-wave rays, and contributions corresponding to "secondary" diffracted body-wave rays. The latter are generated by rays travelling via the crack faces. Thus, the diffracted displacement field at  $Q$  can be represented by

$$u^d = \sum \frac{u^\alpha}{\beta} + \sum \frac{u^\alpha}{\beta\gamma} \quad (1)$$

where

$$\frac{u^\alpha}{\beta} = \text{primary diffracted field} \quad (2)$$

$$\frac{u^\alpha}{\beta\gamma} = \text{secondary diffracted field} \quad (3)$$

In (2) the symbol  $\alpha$  defines the incident ray, i.e.,  $\alpha = L$  or  $\alpha = T$ , while  $\beta$  defines the diffracted ray,  $\beta = L$  or  $\beta = T$ . In (3) the symbol  $\beta$  defines the crack-face ray, i.e.,  $\beta = RS$  (surface-symmetric),  $\beta = RA$  (surface-antisymmetric) or  $\beta = TH$  (horizontally polarized transverse). The symbol  $\gamma$  defines the body-wave rays generated by diffraction of a crack-face ray; thus  $\gamma = L$  or  $\gamma = T$ . The summations in Eq. 1 are carried out over all rays of a particular type passing through  $Q$ .

**Primary diffracted body-wave rays.** For an incident ray of longitudinal motion, the displacement fields on the diffracted body-wave rays are

$$\frac{u^L}{\beta} = e^{i\omega S_\beta/c_\beta} [S_\beta(1+S_\beta/\rho_\beta^L)]^{-1/2} D_\beta^L(\theta; \phi_L, \theta_L) \frac{i^L u^L}{\beta} \quad (4)$$

Here  $u^L$  defines the incident wave at the point of diffraction. In Eq. (4) the superscript  $\beta$  defines the nature of the wave motion on the diffracted rays. Thus we have  $\beta = L$  or  $\beta = T$ . The distances  $S_\beta$  are along the diffracted rays from the point of diffraction  $O$ , to the point of observation. Also

$$\frac{i^L}{\beta} = \text{unit vector,}$$

which relates the displacement directions of the diffracted fields to those of the incident fields, and

$$D_\beta^L(\theta; \phi_L, \theta_L) = \text{diffraction coefficient.}$$

For  $\theta_L = \pi/2$  and  $\phi_L = \pi/2$  the diffraction coefficients have been plotted in Fig. 2. Furthermore,

$$\rho_\beta^L = \text{distance from } O \text{ to caustic.}$$

For an incident longitudinal wave we have

$$\rho_\beta^L = -a \sin^2 \phi_\beta [a(d\phi_\beta/ds) \sin \phi_\beta + \cos \phi_\beta]^{-1} \quad (5)$$

where  $a$  is the radius of curvature of the edge at the point of diffraction,  $s$  is the distance measured along the edge, and  $\delta_\beta$  are the angles between the relevant diffracted rays and the normal to the crack edge, see Fig. 1. The angles  $\phi_L$  and  $\phi_T$  are

related by

$$c_L \cos \phi_T = c_T \cos \phi_L \quad (6)$$

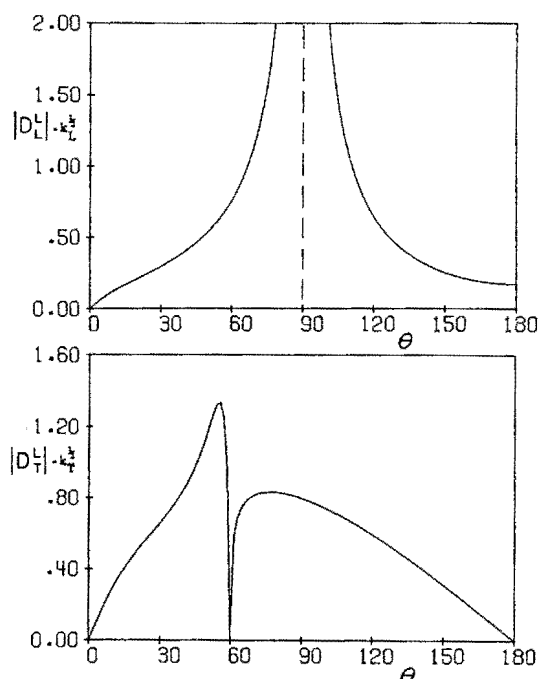


Fig. 2. Absolute values of diffraction coefficients:

$$D_L^L(\theta) = D_L^L(\theta; \pi/2, \pi/2) \text{ and } D_T^L(\theta) = D_T^L(\theta; \pi/2, \pi/2)$$

for Poisson's ratio  $\nu = 1/3$ .

**Diffracted surface wave rays.** Both symmetric and antisymmetric surface wave motions are generated on the faces of the crack. The appearance of surface wave rays in diffraction problems has been discussed in considerable detail in Ref. 4.

**Reflection of surface wave rays.** A surface wave ray which intersects the edge of a crack, gives rise to a ray of reflected surface waves, and to two cones of diffracted body rays. For a surface wave incident on the edge of a semi-infinite crack these reflection and diffraction processes have been studied by Freund<sup>10</sup>. In the spirit of geometrical diffraction theory, we can immediately introduce the appropriate corrections for curvature of the incident wavefront and for curvature of the edge of the crack.

A surface wave ray is reflected such that the angle between the reflected ray and the tangent to the edge is just the same as the angle of incidence between the incident ray and the tangent to the edge. Moreover, rays of symmetric (antisymmetric) surface waves are reflected as rays of symmetric (antisymmetric) surface waves. Expressions for the reflection coefficients can be found in Ref. 4.

**Body-wave rays generated by diffraction of surface-wave rays.** These rays and the associated fields have also been studied in Ref. 4, where express-

ions for the diffraction coefficients have also been presented.

**Comparison of GDT with Numerical Results.** Since GDT is an asymptotic theory, it is not possible to precisely determine a lower limit of validity for  $\omega a/c_L$ . Thus, information on the range of validity of the theory must come by comparison with exact solutions. This has been done in Ref. 5 for diffraction of a normally incident longitudinal wave by a slit. Exact results for this problem have been computed in Ref. 5 by numerically solving a governing singular integral equation which has been derived by Ma<sup>11</sup>.

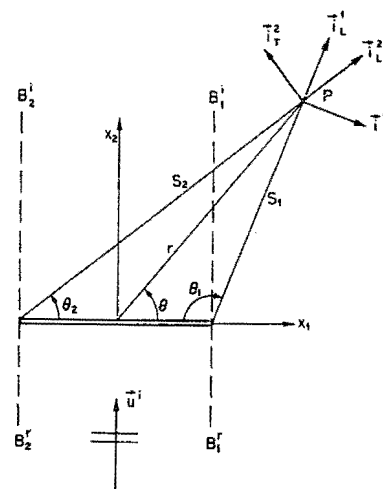


Fig. 3. Geometry for normal incidence of a longitudinal wave on a crack of width  $2a$ .

The crack shown in Fig. 3 can be either a two-dimensional slit or a penny-shaped crack. For the slit, Figs. 4 and 5 show the exact and approximate scattered displacements at  $\theta = 45^\circ$  versus the dimensionless wavenumber ( $k_T a = \omega a/c_T$ ) for two values of  $r/a$ . The solid lines represent GDT solutions which include secondary diffractions. Good agreement is achieved for  $k_T a > 1.5$ , especially for  $r/a = 10$ . Since one must assume at the outset that results produced by an asymptotic theory of the kind presented in this paper are valid only for  $k_T a \gg 1$ , it is quite remarkable that acceptable agreement is already achieved for values of  $k_T a$  as low as 1.5, especially for higher values of  $r/a$ .

For  $k_T a = 5.2$  the contributions from the longitudinal and transverse waves to the displacement components of the scattered field have been plotted separately in Figs. 6 and 7, versus  $\theta$ . The corrections from the uniform asymptotic theory work very well; the curves are smooth and they show satisfactory agreement with the exact results, even though  $D_L^L(\theta)$  is unbounded at the shadow boundary. There are some discrepancies in the contributions from the transverse waves at values of  $\theta$  which appear to correspond to the boundary of the head-wave region.

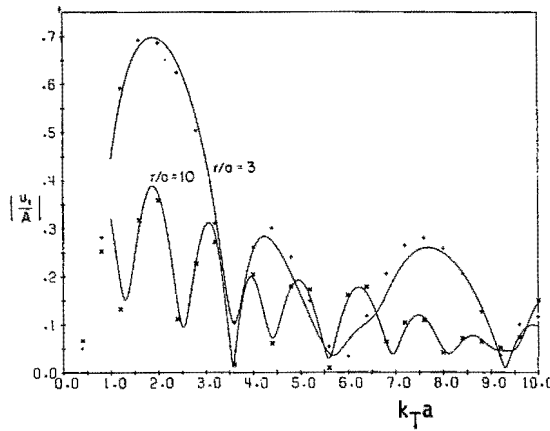


Fig. 4. Comparison of exact scattered  $u_1$ -field (+,x) for a slit with GDT solutions;  $\theta = 45^\circ$ ,  $\nu = 1/3$ .

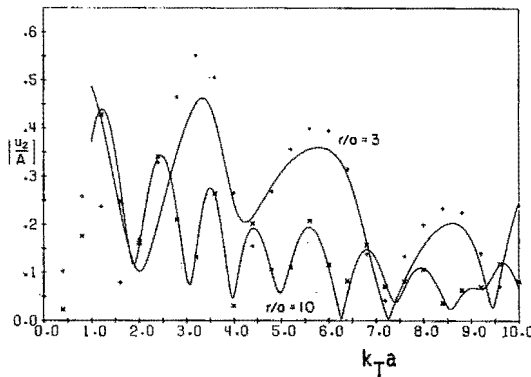


Fig. 5. Comparison of exact scattered  $u_2$ -field (+,x) with GDT solutions;  $\theta = 45^\circ$ ,  $\nu = 1/3$ .

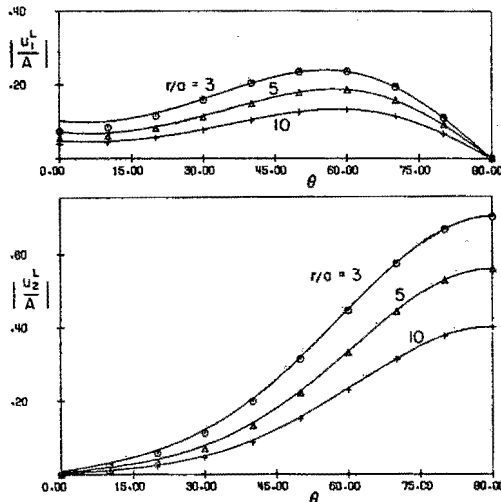


Fig. 6. Comparisons of longitudinal wave components of exact scattered field (0, $\Delta$ ,+) with GDT solutions for  $k_T a = 5.2$  and  $\nu = 1/3$ .

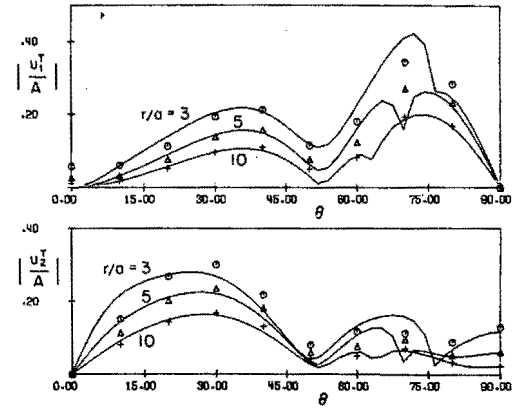


Fig. 7. Comparison of transverse wave components of exact scattered field (0, $\Delta$ ,+) with GDT solutions for  $k_T a = 5.2$  and  $\nu = 1/3$ .

We have also computed exact and GDT results for normal incidence of a longitudinal wave on a penny-shaped crack. These will be presented together with another approximation in the sequel.

**Crack Opening Displacement (COD).** If the crack opening displacement can be adequately approximated, it may be expected that a good approximation to the scattered field can also be obtained by means of a representation theorem for the scattered field. At low frequencies, approximations to the crack opening displacement can be obtained on the basis of quasi-static calculations. At high frequencies  $\Delta u_1$  can be computed on the basis of GDT.

Within the context of the geometrical diffraction theory discussed in this section, the principal contribution to the crack opening displacement comes from the geometrical elastodynamic part of the solution, i.e. from the direct reflection from the crack faces. For normal incidence we have

$$\Delta u_2 = -2 A \quad (7)$$

The body waves associated with the primary diffractions do not generate displacements on the crack faces, except for transverse motions which are polarized in the crack faces. The latter are, however, of order  $O(\omega a/c_L)^{-1/2}$  as compared to (7). Important contributions to the crack opening displacements are, however, generated by the surface wave motions.

For the case of normal incidence of a longitudinal wave on a slit, the absolute value and the phase of the crack opening displacement have been computed for various values of  $k_L a$ , where

$$k_L a = \omega a/c_L \quad (8)$$

At low frequencies (small  $k_L a$ ) the phase is approximately  $\pi/2$ , and the absolute value has an elliptical shape. As  $k_L a$  increases, waveforms develop, which are generated by surface motions of the crack faces. The exact crack opening displacements at high frequencies have been compared with the GDT results. For the slit the comparison is

shown in Fig. 8. Results for normal incidence on a penny-shaped crack are shown in Fig. 9. The displacements according to GDT at the center of the penny-shaped crack, which is a caustic point, have been corrected as discussed in Ref. 4. It is noted that both for the slit and the penny-shaped crack reasonably good agreement was obtained.

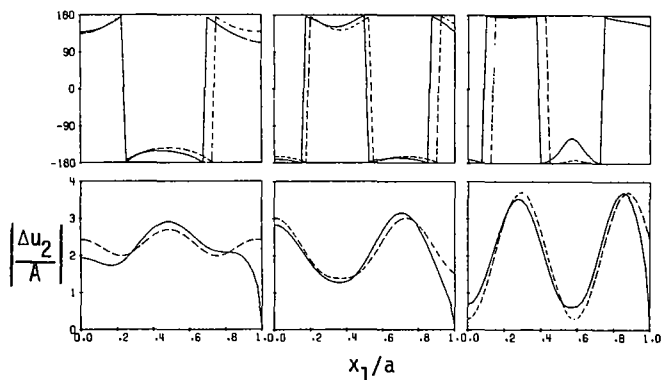


Fig. 8. Phase and  $|\Delta u_2/A|$  versus  $x_1/a$  for  $k_L a = 3, 4$  and  $5$ , for a slit,  $\nu = 1/3$ , - - - GDT, — exact.

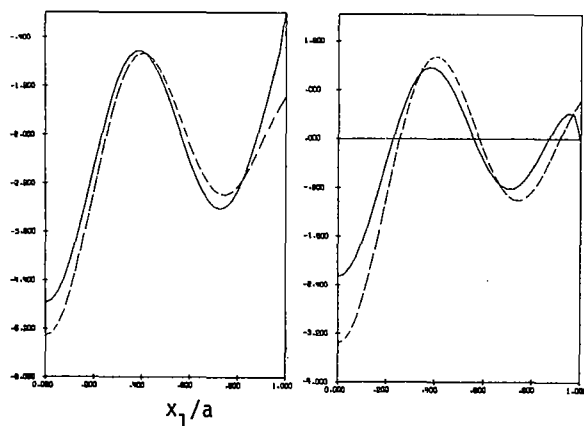


Fig. 9.  $\text{Re}(\Delta u_2/A)$  and  $\text{Im}(\Delta u_2/A)$  for a penny-shaped crack for  $k_L a = 4.4$ ,  $\nu = 1/3$ ; - - - GDT, — exact.

**COD - Representation Theorem Approach.** The results of geometrical diffraction theory are not valid at shadow-boundaries. Moreover, for curved wavefronts and for curved diffracting edges, the cones of diffracted rays have envelopes, at which the rays coalesce and the fields become singular. The envelopes are called caustics. The results of the geometrical theory of diffraction are also not valid near caustics. Even though it is possible to extend the theory to shadow boundaries and caustics, it becomes rather cumbersome. In an alternative approach, the crack opening displacements, which can be computed by GDT as shown earlier, can be used as an input in a representation integral of the scattered field. The scattered displacement fields computed in this manner will be valid at shadow boundaries and at the boundaries of the zones of reflected waves, and there will not be caustic surfaces. Even if  $\Delta u_i$  computed

from GDT should show singularities due to caustics, these singularities will be integrable and the scattered field will be well behaved everywhere.

Let  $\Sigma$  be the area of a flat crack in an unbounded domain. By using the elastodynamic reciprocity relation and the appropriate radiation condition, the displacement components at points not on the crack faces can be expressed by

$$u_k(\underline{x}) = \frac{1}{4\pi r} \int_{\Sigma} \tau_{ij;k}^G \Delta u_i n_j dA \quad (9)$$

where  $\Delta u_i$  is the displacement discontinuity across  $\Sigma$ , and

$$\tau_{ij;k}^G = \text{tensor of rank three}$$

representing the stress components for the basic singular elastodynamic solution. For details on Eq.(9) we refer to Ref. 6.

For the slit results that have been obtained by means of Eq.(9) have been plotted in Fig. 10. In this figure we have also plotted direct GDT results and exact results. The crack opening displacement (COD) plus representation theorem approach is quite good for the displacements from the longitudinal waves, but it requires further improvement for the displacements corresponding to the transverse waves

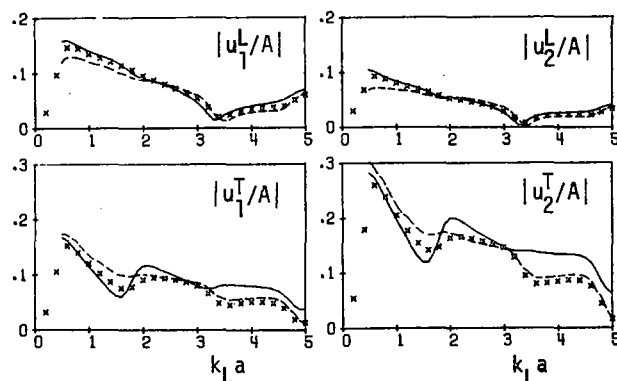


Fig. 10. Contributions to the displacement components from longitudinal and transverse waves, for normal incidence of a longitudinal wave on a slit, for  $\theta = 300^\circ$ ; - - - GDT, — COD + Rep. Thm., x exact results,  $\nu=1/3$ .

Analogous results for normal incidence of a longitudinal wave on a penny-shaped crack are shown in Fig. 11. In this figure we have plotted a further simplification which is obtained when Eq.(9) is replaced by its far-field approximation.

**Error analysis.** It is perhaps surprising that the relatively small errors in the crack opening displacements shown for  $k_L a = 3, 4$ , and  $5$  in Figs.8,9 should still give rise to rather substantial deviations in the diffracted fields, as shown by Figs.10 and 11. The reason is that errors of certain wavelengths in the crack opening displace-

ment are amplified by the representation integral.

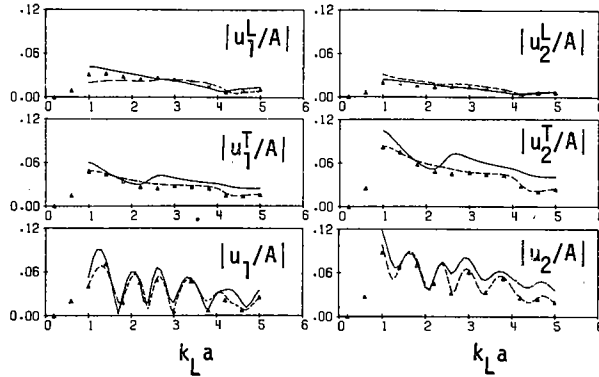


Fig. 11. Contributions to the displacement components from longitudinal and transverse waves, for normal incidence of a longitudinal wave on a penny-shaped crack, for  $\theta = 30^\circ$ ; - - - GDT, — COD + Rep. Thm,  $\Delta$  exact results,  $v=1/4$ .

Let us consider the specific example of the two-dimensional case of normal incidence of a plane longitudinal wave of amplitude  $A$  upon a slit with edges at  $x_1 = \pm a$ ,  $x_2 = 0$ . The far field approximation yields

$$u_k(\underline{x}) \sim i \hat{x}_k [1 - 2(\hat{x}_1 c_T/c_L)^2] J_L^L (8\pi r/k_L)^{-1/2} \exp[i(k_L r + \pi/4)] + 2i \hat{x}_2 (\delta_{2k} - \hat{x}_2 \hat{x}_k) J_L^T (8\pi r/k_T)^{-1/2} \exp[i(k_T r + \pi/4)] \quad (10)$$

where  $\hat{x}_i$  are the components of the unit vector in direction  $\underline{x}$ , and

$$J_\beta^L = - \int_{-a}^a \Delta u_2 \exp(-ik_\beta \hat{x}_1 X) dX \quad (11)$$

The form of the crack opening displacement suggests that  $\Delta u_2$  can be approximated by

$$\Delta u_2 \sim A (-2 + U_R \cos k_R X + \epsilon \cos k X) \quad (12)$$

Here  $-2$  represents the COD due to geometrical elastodynamics,  $U_R \cos k_R X$  represent the crack face motion predicted by GDT, and  $\epsilon$  and  $k$  represent the approximate error from the GE+GDT approximation. Substitution of (12) into (11) yields

$$J_\beta^L = -A a \{ -4 H_\beta(0) + U_R [H_\beta(k_R) + H_\beta(-k_R)] + \epsilon [H_\beta(k) + H_\beta(-k)] \} \quad (13)$$

where

$$H_\beta(k) = [(k - k_\beta \hat{x}_1) a]^{-1} \sin[(k - k_\beta \hat{x}_1) a] \quad (14)$$

We note that  $H_\beta(k)$  takes on its maximum value of unity at  $k = k_\beta \hat{x}_1$ , i.e. for a specific combination of frequency and angle of observation.

Equation (13) also provides insight on the influence of the surface wave terms on the dif-

fracted field. Near  $x_1 = 0$  (i.e.,  $\theta = \pi/2, 3\pi/2$ ) the contribution from the GE term dominates the contribution from the surface waves in both the longitudinal and transverse fields, while near  $x_1 = 1$  ( $\theta = 0, \pi$ ) the contribution from the surface waves dominates the transverse field, since  $k_T/k_R$  (where  $k_R = \omega a/c_R$ ) is generally slightly less than unity.

#### SOME COMMENTS ON THE INVERSE PROBLEM

So far, this paper has been concerned with the direct problem, that is, the computation of the scattered field when the size, shape and orientation of the crack are known. We will conclude with a few comments on the inverse problem for plane waves incident on slits and penny-shaped cracks, for the special case that the diffracted field is symmetric relative to the plane through the  $x_1$  and  $x_2$  axes. For both the slit and the penny-shaped crack the geometry in the plane of symmetry is then essentially as shown in Fig.3, except that the incident wave is under an angle, say  $\theta_0$ , with the  $x_1$  axis. For a given point of observation, say the point P in Fig.3, the unknowns then are  $\theta_0$ ,  $a$  and  $\theta$ .

In experiments the nature of diffracted signals is largely determined by their arrival times. Since the first arriving signal is longitudinal, it is often possible to gate out the purely longitudinal diffracted signals from subsequent signals. The frequency spectrum of these longitudinal signals contains a considerable amount of information on the crack. Upon division by the frequency spectrum of the incident wave, one obtains, in fact, the amplitudes and phases corresponding to single harmonic waves at high frequencies. Comparison of this experimental information with the analytical fields on the primary diffracted body wave rays provides a way to solve the inverse problem.

For the geometry discussed here the displacement fields on the primary diffracted body wave rays follow from Eq.(4) as

$$u_L^L = e^{i\omega S_L/c_L} [S_L (1 + S_L/\rho_L^L)]^{-1/2} D_L^L(\theta; \pi/2, \theta_L) i_L^L u_L^L \quad (15)$$

It is convenient to define a dimensionless diffraction coefficient as

$$\overline{D}_L(\theta; \theta_L) = k_L^{1/2} e^{-i\pi/4} D_L^L(\theta; \pi/2, \theta_L) \quad (16)$$

The angles of incidence at the two points of diffraction are  $\theta_L = \theta_0$  and  $\theta_L = \pi - \theta_0$ , respectively. If the point of observation is sufficiently far from the crack, we have, see Fig.3

$$S_{L1} \sim r - a \cos \theta \quad (17)$$

$$S_{L2} \sim r + a \cos \theta \quad (18)$$

$$\theta_2 \sim \pi - \theta_1 \sim \theta \quad (19)$$

$$(i_L^L)_1 \sim (i_L^L)_2 \sim i_r \quad (20)$$

$$(u_L^L)_1 \sim u_0^L \exp(ik_L a \cos \theta_0) \quad (21)$$

$$(U_L^L)_2 \sim U_0^L \exp(-ik_L a \cos \theta_0) \quad (22)$$

where  $U_L^L$  defines the incident wave at the center of the crack. Adding the primary diffracted longitudinal fields from the points 1 and 2, we obtain

$$(ud)_L \sim U_0^L (k_L r)^{-1/2} (1+r/\rho_L)^{-1/2} e^{i\pi/4} e^{ik_L r} F \quad (23)$$

where

$$F = \bar{D}_L(\pi-\theta; \pi-\theta_0) e^{-ik_L a(\cos\theta - \cos\theta_0)} + \bar{D}_L(\theta; \theta_0) e^{ik_L a(\cos\theta - \cos\theta_0)} \quad (24)$$

Of particular interest is the absolute magnitude of  $F$ :

$$|F| = \{ [\bar{D}_L(\pi-\theta; \pi-\theta_0)]^2 + [\bar{D}_L(\theta; \theta_0)]^2 + 2 \bar{D}_L(\pi-\theta; \pi-\theta_0) \bar{D}_L(\theta; \theta_0) \cos[2k_L a(\cos\theta - \cos\theta_0)] \}^{1/2} \quad (25)$$

This result implies that the amplitude of the primary diffracted field is modulated with respect to  $k_L$ , with period

$$P = \pi / a | \cos \theta - \cos \theta_0 | \quad (26)$$

An analogous expression can be derived for the primary diffracted transverse field. From the practical point of view this latter expression is of less importance, because measurements of the transverse field usually are polluted by other signals.

Figure 12 shows the amplitude envelopes of the radial displacements corresponding to the primary longitudinal rays at three positions  $\theta = 30^\circ$ ,  $45^\circ$  and  $60^\circ$  for the case of normal incidence of a longitudinal wave on a penny-shaped crack. The three curves show the characteristic behavior discussed in the previous paragraph, and it is easily checked that the increment  $\Delta k_L a$  between peaks indeed equals  $\pi/\cos\theta$  (note that  $\theta_0 = 90^\circ$ ).

Experimental results also show the modulation displayed in Fig.12, see e.g. Ref.12. The unknowns in Eq.(26) are  $a$ ,  $\theta$  and  $\theta_0$ . Suppose we have four points of observation  $Q_0$ ,  $Q_1$ ,  $Q_2$  and  $Q_3$ , on a straight line in the plane shown in Fig.3, distances  $\ell_1$ ,  $\ell_2$ , and  $\ell_3$  apart. The angles  $\theta$  corresponding to  $Q_1$ ,  $Q_2$  and  $Q_3$  are  $\theta_1$ ,  $\theta_2$  and  $\theta_3$ , respectively. The arrival times of the first longitudinal diffracted signals are denoted by  $t_0$ ,  $t_1$ ,  $t_2$  and  $t_3$ , respectively. It then easily follows that

$$\begin{aligned} \gamma_1 = \theta_2 - \theta_1 &= \cos^{-1} [c_L(t_2 - t_1)/\ell_2] - \cos^{-1} [c_L(t_1 - t_0)/\ell_1] \\ \gamma_2 = \theta_3 - \theta_2 &= \cos^{-1} [c_L(t_3 - t_2)/\ell_3] - \cos^{-1} [c_L(t_2 - t_1)/\ell_2] \end{aligned}$$

If  $P_1$ ,  $P_2$  and  $P_3$  have been measured at  $Q_1$ ,  $Q_2$  and  $Q_3$ , we then have five equations for the five unknowns  $a$ ,  $\theta_0$ ,  $\theta_1$ ,  $\theta_2$  and  $\theta_3$ , which can easily be solved.

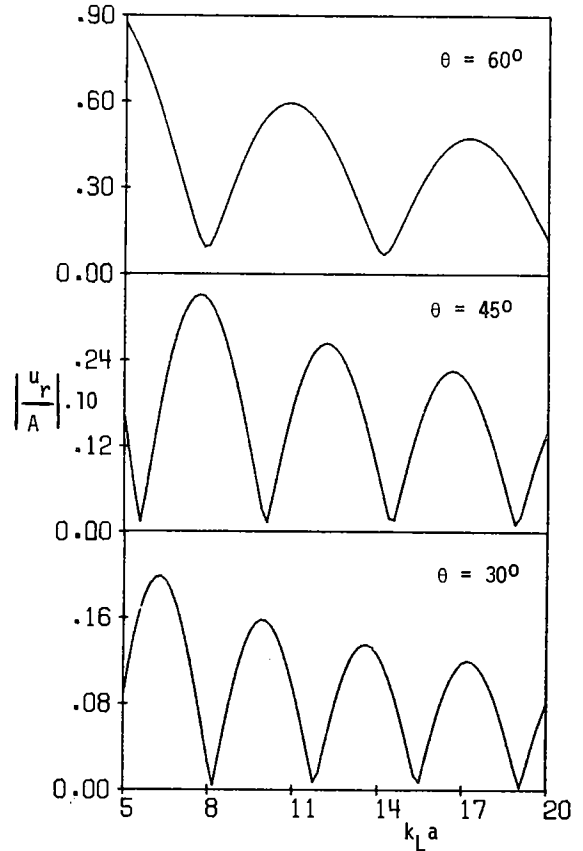


Fig. 12. Amplitude envelopes versus  $k_L a$  for  $r/a = 10$  and  $\nu = 1/4$ .

#### CONCLUDING COMMENTS

For normal incidence of longitudinal waves on slits and penny-shaped cracks it has been shown in this paper by comparison with exact numerical results that geometrical diffraction theory (corrected at shadow boundaries and caustics) provides surprisingly good results at relatively small values of the frequency (say  $k_L a > 1.5$ ) and relatively close to the crack (say  $r/a > 5$ ). For more complicated geometries (elliptical cracks) the corrections at shadow boundaries and caustics become, however, more cumbersome. We have, therefore, also explored an alternative approach in which the crack opening displacement, which can be computed by GDT with relative ease, is used as an input in an exact or approximate representation integral for the scattered field. The scattered displacement fields computed in this manner are valid at shadow boundaries and they do not have caustic surfaces. The crack opening displacement computed by GDT may have singular points or curves, but the singularities are integrable. Comparison of the results obtained by this hybrid approach with exact results shows good agreement for the longitudinal wave

contributions, but some improvements are desirable for the transverse wave contributions.

The simple structure of the high frequency longitudinal wave results suggests a simple approach to the inverse problem, which has been briefly discussed.

#### ACKNOWLEDGEMENT

The results presented here were obtained in the course of research sponsored by the Center for Advanced NDE operated by the Science Center, Rockwell International, for the Advanced Research Project Agency and the Air Force Materials Laboratory under Contract No. F33615-74-C-5180.

#### REFERENCES

1. Karal, F. C., and Keller, J. B., "Elastic Wave Propagation in Homogeneous and Inhomogeneous Media," J. Acoust. Soc. Amer., 31, 1959, p. 694.
2. Resende, E., "Propagation Reflection and Diffraction of Elastic Waves," Ph.D. Dissertation, New York University, 1963.
3. Achenbach, J. D., and Gautesen, A.K., "Geometrical Theory of Diffraction for Three-D Elastodynamics," J. Acoust. Soc. Amer., 61, 1976, pp. 413-421.
4. Gautesen, A. K., Achenbach, J. D., and McMaken, H., "Surface Wave Rays in Elastodynamic Diffraction by Cracks," J. Acoust. Soc. Amer., 63, 1978, pp. 1824-1831.
5. Achenbach, J. D., Gautesen, A. K., and McMaken, H., "Application of Elastodynamic Ray Theory to Diffraction by Cracks," Modern Problems in Elastic Wave Propagation, Wiley-Interscience, New York, 1978.
6. Achenbach, J. D., Gautesen, A. K., and McMaken, H., "Diffraction of Elastic Waves by Cracks - Analytical Results," in Elastic Waves and Non-Destructive Testing of Materials, American Society of Mechanical Engineers, in press, 1978.
7. Keller, J. B., "A Geometrical Theory of Diffraction," Calculus of Variations and Its Applications, McGraw-Hill, 1958.
8. Keller, J. B., "Diffraction by an Aperture," J. Appl. Phys., 28, 1957, pp. 426-444.
9. Kouyoumdjian, R. G., "The Geometrical Theory of Diffraction and its Application," Numerical and Asymptotic Techniques in Electromagnetics, Springer-Verlag, New York, 1975.
10. Freund, L. B., "The Oblique Reflection of a Rayleigh Wave from a Crack Tip," Int. J. Solids Structures 7, 1971, p. 1199.
11. Mal, A. K., "Interaction of Elastic Waves with a Griffith Crack," Int. J. Eng. Sc. 8, 1970, p. 769.
12. Adler, L., "Identification of Flaws from Scattered Ultrasonic Fields as Measured at a Planar Surface," Interdisciplinary Program for Quantitative Flaw Definition, Rockwell International, September 1977. pp. 122-158.



## DISCUSSION

Tom Kincaid (General Electric): I have to lead up to my question with a little preamble. I tried to use this theory for cracks on steam turbines. When I did that I said, "Well, it is going to be easy because those 2 corners are going to radiate. I am going to end up getting a nice zero in the spectrum which will tell me the length of the crack," and we spent several months working on the theory and then we took a look at some cracks. The first thing I noticed was that a crack is not as flat as you assumed here. A crack is ragged in the middle with the main reflections coming off those ragged surfaces that are oriented in the direction of observation. I think that we will have to consider we are going to have such real cracks. I would like to get some comments from you on how we are going to handle the real problem.

J. D. Achenbach (Northwestern University): Yes, you are absolutely correct, this is a problem. Naturally, the solution depends upon the direction of observation. If you observe from behind the crack, you can deal with the crack in the above fashion. The problem you are talking about is in interpreting the back reflections from rough surfaces

Tom Kincaid: That is correct. In general, one receives a very complicated spectrum. Only in a very few cases does this spectrum have any similarity with the one you are talking about. You are saying that by observing from behind the crack all those ragged surfaces are basically invisible. That does not really avoid the problem: Frequently you cannot inspect the part so as to avoid the problem. I am trying to make an appeal to this group to understand that we need solutions that are not critically dependent on the crack geometry. These solutions should not depend on the fact that the crack is a smooth mirror with corners. To be useful, research will have to take these facts into consideration. The raggedness of the fracture surface is a statistical problem, in part, that we have to solve to be able to perform the inversion.

J. D. Achenbach: I agree with you, that is the problem. We should get some idea on the relative magnitudes of the characteristic dimensions of the roughness.

Tom Kincaid: Using micrographs you can get a good idea about the roughness.

J. D. Achenbach: I think the incident wavelength will have to be of the same order of magnitude as the crack, but it certainly has to be much larger than the crack's roughness. Certainly, if the roughness is of the same magnitude as the acoustic wavelength, you get the kind of problem you are alluding to.

Gordon Kino (Stanford University): Perhaps I could try and bridge this gap a little. We have been using an imaging system to look at cracks. In fact, we showed some pictures last year. What you see with an imaging system, illuminating an elox crack, is a smooth crack with sharp fronts, as Dr. Achenbach pointed out.

Using a real crack with real roughness you see scattered acoustic energy from everywhere, as Mr. Kincaid points out. I would suggest that as the theoretical techniques keep on developing and as we will learn to do the inverse process properly (which in one way is by imaging, the other way is essentially by mathematical techniques), we will not only see its front but we will see some information from all along the fracture surface. We will still get the length which is what we want to know, basically. I think you have to allow the theoreticians time because what they have got to do is the simplest problem first and then work up to the complicated ones.

Bernard Tittmann (Science Center): I would like to make a comment. Tomorrow morning I will show data on a real crack in ceramics and I will use a diffraction theory, similar to that by Young, to analyze the radiation pattern from a crack and I will show that this theory works. This pattern is as clean as that of an elox notch, but it does yield crack length information, as Gordon Kino has pointed out. I agree with Dr. Kino. I think we can achieve the solution to the problem.

Vernon Newhouse (Purdue University): I would like to plead with the theorists to stop casting their results in the time domain which, of course, is just a question of Fourier transforming the spectral results. It is, naturally, a lot more convenient to measure arrival times than to start analyzing a frequency spectrum and, furthermore, it may simplify the mathematics. If you are looking at a crack and measure arrival time of the first array and the last array at several different points, you probably will get information in a simpler way than you can from spectral results even when the crack is distorted.

J. D. Achenbach: I agree. From my point of view the time domain is just as good as the frequency domain. In fact, in some of our work we are trying to combine time domain and frequency domain considerations. Not being an experimentalist, I thought that even though there are definite peaks in the time domain it was still quite easy to make slight errors in the interpretation. On the other hand, if you take a frequency spectrum, where you integrate, you don't run into danger of making a significant error. Otherwise, I will go along with you.

W. Sachse (Cornell University): One comment, time domain is the approach that we are using in studying scattering of cracks experimentally.

John Zurbrick (General Electric): We grow cracks that we ask our inspectors to find for us. There is something that I have observed over the last couple of years in this program that is quite interesting to note and I think it tends to bridge some of the gaps that we are discussing. We have done a lot of acoustical microscope work, we have done a lot of imaging of flaws in real time and the time domain and we have done adaptive learning network experiments. The point is this. We are looking heavily at the surface convolutions of a crack and the indications that are or are not coming from the center. The center of the crack isn't really what causes the part to fail. It really is the plastic zone around the crack which has a shape that is very close to an oblate spheroid. I like the approach of looking at hollow oblate spheroids, but let's keep in mind that a fatigue crack, together with this plastic zone around it, reflects, refracts, mode converts, etc. I would encourage this kind of an approach. We are not just looking at a hole. We are looking for the degraded material around the crack tip. Actually, you can see certain similarities to an oblate spheroid because the crack grew from the middle to its present tip.

J. D. Achenbach: I don't think that the method I described would be suitable to describe this situation.

Earl Duback (General Dynamics): My background is in sonar and acoustics and I worked on problems similar to the one you are describing, a multi path situation. If you are able to obtain a cross correlation function and your signal is frequency-wise not broad enough, you can separate out the various acoustic paths. If you are looking at the amplitude information versus frequency, and if you look at the phase, you will find ripples in the phase. By zeroing out the signals in the correlation function from the various paths, you obtain nice linear phase information that will show you the energy coming along the different paths.

J. D. Achenbach: I am aware of what has been achieved along those lines in your field, and we would like to take similar approaches.